Chapter 2
Methodology of Design and Characterization of Bionano- and Nanorobotic Devices

1 Introduction

Nanorobotics is an emerging interdisciplinary technology area raising new scientific challenges and promising revolutionary advancements in applications such as medicine, biology and industrial manufacturing. Nanorobots could be defined as intelligent systems with overall dimensions at or below the micrometer range that are made of assemblies of nanoscale passive or active components with individual dimensions ranging between 1 to 100 nm. Nanorobots would be able to perform at least one of the following actions: actuation, sensing, signaling, information, processing, intelligence, swarm behavior at the nano scale. Bio-nanorobots are nanorobots using various biological elements—whose function at the cellular and sub-cellular level creates a motion, force or a signal—as machine components that perform the same function in response to a biological stimuli.

Since the development of these molecular machines is a relatively new research field, the derivation of computational to model and analyze their performance is still at an early stage. To design high-performance nanorobotic structures and systems, fundamental, applied, and experimental research must be performed. One of the most challenging problems in bionano- and nanorobotic design is the topology-architecture-configuration synthesis, system integration and optimization. Towards this end, the selection of analytical and numerical methods, computation algorithms, model accuracy and simulation environment is crucial for virtual prototyping and optimization at an early-stage of development. Indeed, modeling allows the designer to devise novel phenomena and new operational principles guaranteeing synthesis of nanorobotic components, subsystems and systems with enhanced functionalities. The computational studies aim at developing models that can be used in understanding the mechanism of the proposed robotic nanostructure, in predicting its feasibility and performance in terms of energy, force, speed, and other kinematic and dynamic criteria as well as perform optimal design procedures to identify the optimal structure performances. Many novel concepts and designs have been first proposed based on modeling and simulations, and then were followed by their realization or verification through experiments.

M. Hamdi, A. Ferreira, *Design, Modeling and Characterization of Bio-Nanorobotic Systems*,
DOI 10.1007/978-90-481-3180-8_2, © Springer Science+Business Media B.V. 2011

In this chapter we investigated computational nanotechnology methodologies, i.e., physics-, biology- and chemistry-based modeling and simulation, dedicated to the design and optimization of bio-nano structures. An attempt has been made to emphasize the paradigm of how computational nanotechnology can be used to not only understand and characterize the systems under experimental investigation (termed, *co-prototyping design*), but also as to how predictions can be made for novel applications (termed, *interactive multiscale design*), because there is a strong coupling between the structural, mechanical, chemical and biological properties at multiple length–time-scale. Two prototyping methodologies are proposed and discussed:

1. *Interactive multiscale design*: The proposed multiscale methodology hierarchical simulation techniques considers virtual reality techniques coupled to computational quantum mechanics, molecular dynamics and continuum models. The interactive multiscale simulation methodology allows to simulate, analyze, model, and visualizes the complex architecture and interactions of biological nanorobotic components. The goal is to prototype virtually bio-nanorobotic systems and control their movements in their biological environment before experimentation.
2. *Co-prototyping design*: The proposed co-prototyping methodology is an approach to the development of nanostructures composed of experimental characterization and computational nanotechnology modeling (ab-initio and molecular dynamics simulation methods) towards optimized, reliable and reusable nanorobotic structures.

This chapter begins with a section (Sect. 2) describing the technical and simulation aspects of the interactive virtual multiscale simulation system. First, we consider the hardware configuration and virtual reality input devices, and then the multiscale modeling methods and prototyping methodology. Then, a section (Sect. 3) presents the co-prototyping methodology and simulation aspects, including requirements on the use of semi- and empirical modeling methods. Concluding remarks are given in Sect. 4.

2 Design and Characterization Methodology of Biological Nanodevices

Objective

Recent advances in understanding how biomolecular motors work has raised the possibility that they might find applications as protein-based nanomachines. For example, they could be used as molecule-sized robots that are able to apply forces and manipulate objects in the nanoscale world. Thus biomolecular motors could form the basis of bottom-up approaches for constructing active structuring and maintenance at the nanometer scale. Protein is the most versatile of the natural bionanomachines. As an example, the most familiar motor is the protein myosin [1]

or dynein [2] which moves along filaments, formed through the protein actin, to drive the contraction of muscles. In addition, there are compliance devices such as spring-like proteins called fibronectin [3] and vorticellids [4], as well as synthetic contractile plant polymers [5] which can act as compliant joints in molecule-size robotic systems. The idea is to use biomolecular motors as the actuators of such bionanorobots, where the structural elements are carbon nanotubes (CNTs), while the joints are formed by appropriately designed biological spring elements [6]. To achieve these long-term goals, prototyping tools based on molecular dynamics (MD) simulators should be developed in order to understand the molecular mechanics of proteins and develop dynamic and kinematic models to study their performances and control aspects. The ability to visualize the atom-to-atom interaction in real-time and see the results in a fully immersive 3D environment is an additional feature of such simulations [7]. Virtual reality (VR) technology is applied here, which not only provides immersive visualization but also gives an added functionality of CAD-based design, simulation, navigation and interactive manipulation of molecular graphical objects. Using virtual biological environments, the operator can design and characterize through physical simulation the behavior of bio-nanorobots. Adding haptic interaction, the operator can explore and prevent the problems of molecular robots in their native environment. Based on VR technology and MD simulators, our long-term goal is to prototype virtually bio-nanorobotic systems and control their movements in their biological environment.

Overall CAD-design Methodology

Considering the above mentioned research issues, we decided to adopt VR technologies coupled to computational molecular dynamics and quantum molecular dynamics to simulate, analyze, model, and visualizes the complex architecture and interactions of bio-nanorobotic components. Real-time exploration is what attracts researchers to develop man-machine interfaces for nanoscale manipulation that use haptic display technologies. The developed simulation system presented in Fig. 2.2 permits manipulation, connection and assembly of bio-nanorobotic components in molecular dynamics simulation with real-time VR devices such as stereo glasses, 3D trackers, force-feedback devices and 3D graphical display.

Nanoassembly methodology requires to address the assembly process systematically to design it optimally. Two major assembly processes are currently employed at the nanoscale. Robotic nanoassembly, much like its macroscopic counterpart, involves positioning and joining of components. Nanocomponents are positioned by using the atomic force microscope (AFM) as a robot, essentially by pushing the components mechanically and joining them chemically, by using linkers such as DNA complementary strands, or by depositing additional material over the templates defined by the nanocomponents [8, 9]. Mass production is best approached by programmed self-assembly, using scaffolds designed by algorithmic methods. Several self-assembly approaches have been proposed based on various forces such

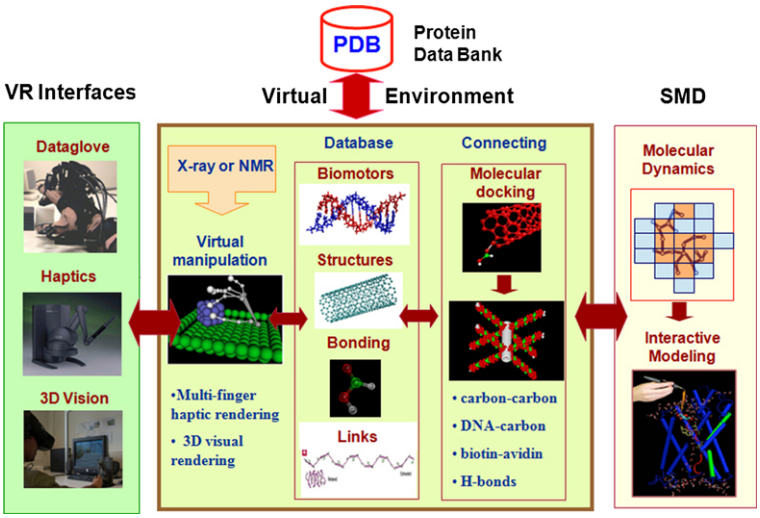


Fig. 2.1 Design methodology of bio-nanostructures

as capillary force, hydrophobic force, electrostatic force and so on [10, 11]. The controlled nanoassembly approach is based on hierarchical theoretical and computational assembly methods depicted on the flowchart shown in Fig. 2.2:

1. To connect and assemble interactively the molecular components of the bio-nanorobotic structure through a data glove which can be displayed in the virtual environment as a mapping of hand. It is composed of fully enclosed fiber optic bend sensors that provides up to 18 high-accuracy joint-angle measurements allowing to capture all assembly hand postures.
2. To virtually steer the protein molecules using a haptic device. The haptic device is virtually bound to an atom of a conformationally stable subset of the molecule. This system would allow applying stretching, shearing and bending mechanical constraints on the protein.
3. To distinguish possible conformational paths, feel the energy barriers associated with each path and choose the optimal path/strategy.
4. To control the interaction mechanism in a solvent. Protein folding and unfolding can be controlled by assessing the influence of pH value, temperature, electron density or salt concentration.

The software architecture is composed of three software modules: (i) a haptic device module controlled by a computer that generates the force environment, (ii) an interactive molecular environment (IME) module for manipulation, attachment and assembly of nanocomponents in 3-D virtual world and (iii) a molecular dynamics (MD) module for determining the effects of force application.

As shown in Fig. 2.2, steering forces are issued from the haptic device which measures a user's hand position and exerts a precisely controlled force on the hand in order to apply different mechanical constraints, force and energy fields on the

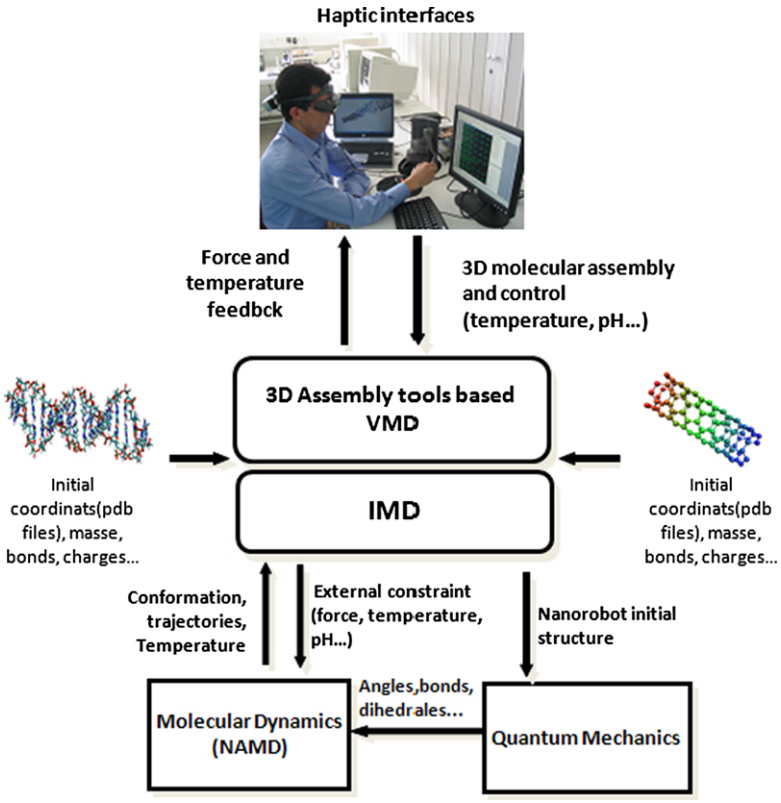


Fig. 2.2 Basic concept of virtual environment and haptics technology coupled to multiphysics computational methods for bio-nanorobotic design

virtual model in order to prototype bionanorobotic components. The haptics module sends command data (position, velocity, force) and receives force feedback signals from the IME module.

The main role of the interactive molecular environment module (IME) module is to gather the nanorobotic components (proteins, DNA, CNT, graphite, ...) in a one 3-D representative space called visual molecular dynamics (VMD) [12]. VMD software is a molecular visualization program for displaying, animating and analyzing large bimolecular systems using 3-D graphics and built-in scripting. The VRPN software package [13] was used to connect VMD to the PHANToM Desktop device. The Data Glove input device is also supported by VRPN. The user manipulates in an intuitive way the attachment and assembly of the different molecular components within VMD environment. As the linkers and/or connectors between multidomain proteins are not always clear during complex assemblies, *Pdbswiss* software allows the analysis of structural protein and/or nanostructure misalignments (rotation, translation, orientation). When the 3-D structures are aligned, the molecular

attachment between the different components is achieved via *VegaZZ* software.[1] Finally, the a molecular structure will be generated, associated to the CAD-designed bio-nano robotic structure: initial coordinates, force field parameters, structure solvation and ionization.

These data are sent to the molecular dynamics (MD) module through a communication protocol named interactive molecular dynamics (IMD) [14]. The IMD interface consists of a small set of C-callable functions which can be adapted to any molecular dynamics and/or visualization program. Periodically, VMD checks for a coordinate set from the MD program, updates the representation geometry if a new coordinate set was received, redraws the screen, and updates the restraint position of the haptic device. If the user has applied a force through the haptic device, VMD routes this force to NAMD2, which then integrates the force into the equations of motion for the molecule. Updates to the haptic restraint point are made when VMD receives a new coordinate set from NAMD2 software; while awaiting an update, the haptic server applies smooth feedback forces based on the most recent restraint point position.

The main program of the computational is NAMD2 [15], a fast, scalable, program which implements the popular CHARMM27 force field [16] for molecular dynamics. The absolute speed of NAMD2 is an essential ingredient of a responsive interactive system. It runs on a parallel cluster composed of 10 Pentium IV–4.1 GHz personal computers. NAMD's scalability enables us to use the computational module to study large bio-nanorobotic structures as well as small ones, given enough computational power. These computational resources allow the simulation of systems containing several thousand atoms at a speed sufficient for interaction ($\sim$400 Hz).

When size goes down to nanoscale or molecular scale, besides the widely known spatial and temporal multiscale problems, new physical properties and coupling effects between mechanical motion and physical, biochemical properties may become dominant, and multiphysics-scale problems arise. Design of bio-nanorobotic systems is a complex and need research on modeling and simulation of physical, chemical, mechanical and biological systems at the nanoscale. These include techniques that mainly cover the range of multidisciplines from atomistic mechanics to continuum mechanics: quantum mechanics, multi-particle simulation, molecular simulation, continuum-based models, stochastic methods, and nanomechanics. Approaches that make use of more than one such technique and focus on their integration play an important role in this effort.

Current proposed multiscale models for non-organic materials do not integrate the hierarchical design and focus mainly in the multiscale modeling of single components, such as carbon nanotubes (CNTs) [17] or electronic materials [18]. Some multiphysics models have been proposed but the proposed models does not take into consideration all physical interactions, such as quantum mechanics (QM), nanomechanics (NM) [19], or multiphysics parametrization in order to ensure connection

[1] http://www.ddl.unimi.it/vega/i

between length scales (from atomistic to macroscopic) [20]. Computational methods based on molecular dynamics (MD) are of great interest for investigations of structure, function, and dynamics of structural biology from the atomic level to the macromolecular level [21]. The fundamental issue is to integrate models addressing phenomena from the level of individual gene and cell features through tissue and organ models. Recent approaches are combining multiscale modeling of macromolecular conformational changes to concepts from rigidity and elastic network theory [22]. A good example is given in [23] where the structural dynamics of the lac repressor-DNA complex is described by all-atom molecular dynamics and continuous elastic ribbon. Still, due to their size, biomolecular systems characterized by computational methods like molecular dynamics, are often beyond the reach of real-time feedback for control.

The objective of our work is to demonstrate a framework that couple multiscale, multiphysics and virtual reality advanced techniques for the design and modeling of bio-nanorobotic systems. A three-level modeling paradigm was developed for this purpose. Quantum mechanics (QM) for designed components parametrization, molecular dynamics (MD) for mechanical properties characterization and continuum-model (CM) for system simulation.

Virtual Reality Interfaces

The application of advanced virtual reality (VR) techniques in bio-nanotechnology allowed to study, simulate, visualize and interact with molecular biology, genomics, proteomics, structural and computational biology. As far we know, only basic molecular elements have been studied until now. As a perspective of these developments, VR-based technology could be used for the biomolecular robot design (see Fig. 2.3). The multiscale prototyping simulator that is capable of supporting VR devices such as stereo glasses, 3D trackers, dataglove and force-feedback (haptic) devices is of great interest. This development effort will permit operators to build models, combine atomic and volumetric data, and perform manipulation, assembly, steering forces interactively within a single computational environment.

Haptic Interaction

In this section, we describe our design and implementation of a communication scheme connecting a force feedback device, visualization program, and simulation engine. The incorporation of virtual reality into molecular science has only just begun. Several types of software for displaying 3D models of bio-molecules have been developed. Most of these programs use Virtual Reality Modeling Language (VRML). Few attempts to use force feedback have been investigated. Force feedback technology for protein-ligand docking have been used, i.e., local-minima force field minimization using haptic interaction [24, 25], steered molecular dynamics for

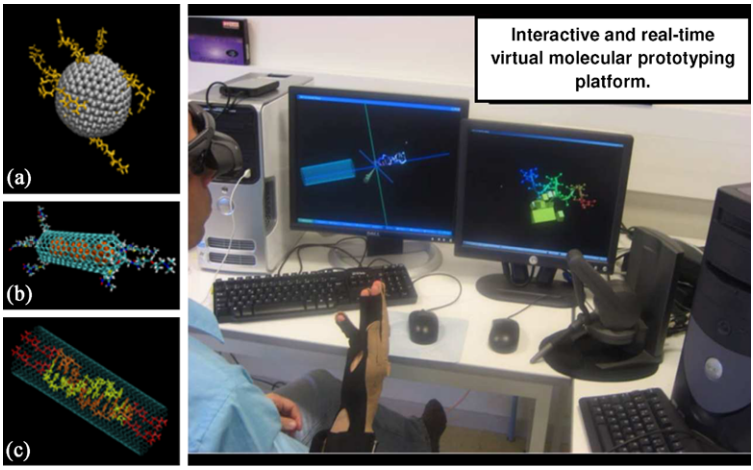


Fig. 2.3 *Left*: Pictures (**a**)–(**c**) show some bio-nanorobotic structure designs. *Right*: Picture (**d**) shows the experimental interactive simulation platform using virtual reality interfaces. In the virtual molecular dynamics (VMD) environment, the user applies forces to bio-nanorobotic structures in the simulation via a force-feedback haptic interface while manipulation is performed through a virtual hand. The headtracker is mounted on a pair of shutter glasses for operator immersion

protein stretching [26, 27] or feeling attractive and repulsive forces when screening molecules [28, 29]. The Interactive Molecular Dynamics (IMD) [14] permits manipulation of molecules in molecular dynamics simulations with real-time force feedback and graphical display. It provides interactive steering molecular dynamics calculations by adding user-specified external forces into the computation on the fly. Steering implies that the user is able to 'tug' an atom or a group of atoms towards a desired target position. Communication is achieved through an efficient socket connection between the visualization program (VMD) and a molecular dynamics program (NAMD) running on single or multiple machines.

A natural force feedback interface for molecular steering is provided by an haptic device (SensAble Technologies PHANToM Desktop interface). The physical forces generated by the user's hand are translated into forces on simulated atoms. Three scaling parameters define the relationship between the virtual haptic environment and the simulation environment.

- α, is the ratio of wall clock time required for a molecular dynamics timestep to the physical simulation time, and is presently at least 10^{12}.
- β, is the amount by which forces applied by the user are scaled before being applied to atoms in the simulation.
- γ, is the factor that scaled up atomic coordinates to be perceptible to humans.

These parameters have certain limitations. First, α and β can be set to any value the user desires; however, the value of β has important implications for the sensitivity and responsiveness of the IMD module. Second, β is limited by the workspace

of the haptic device, although one could in practice focus on a small part of the simulation region in order to increase the spatial resolution of the haptic interface.

Let us to derive a model rendering the haptic force exerted on the user's hand. In the user-haptic coordinate system, let F_{haptic} be the force exerted by user's hand on the haptic device. The particle experiences a force $\beta . F_{haptic}$, taking into account the scaling of applied forces.

We can relate the dynamics of the particle as perceived in the haptic environment to the dynamics of the particle in the simulation. Let x and t be the space and time coordinate, respectively, of the particle in the haptic environment, and χ and τ be the corresponding simulation variables. The dynamics of an otherwise free particle in the simulation are given by

$$m\frac{d^2\chi}{d\tau^2} = \beta F_{haptic} = m\frac{\alpha^2}{\gamma}\frac{d^2x}{dt^2}. \tag{2.1}$$

The user interprets the motion of the particle in terms of F_{haptic} and an effective mass m^*, defined by

$$F_{haptic} = m^*\frac{d^2x}{dt^2}. \tag{2.2}$$

Combining (2.1) and (2.2), we arrive at an expression for the effective mass in terms of the actual mass of the particle and the scaling parameters:

$$m^* = m\frac{\alpha^2}{\gamma\beta}. \tag{2.3}$$

Now, consider the special case in which the applied force is proportional to the distance of the particle in the virtual environment from a restraint point that moves with the haptic controller. In this case $F_{haptic} = -kx$, where k is the spring constant defining the strength of the restraint. The atom experiences an external force $\beta kx = k\beta\gamma\chi$. If the particle is also subject to a potential U due to the presence of other atoms in the system, the dynamics of the particle will be given by

$$m\frac{d^2\chi}{d\tau^2} = -k\beta\chi\gamma - \frac{dU}{d\chi}. \tag{2.4}$$

Equations (2.3) and (2.4) together describe the interplay of the scaling parameters in determining the environment experienced by the user in IMD module. In order for the system to respond to applied forces, m^* must be reasonably small, i.e. a few kilograms, since the maximum force that can be exerted by modern haptic devices is ~1–10 N. As illustration, Fig. 2.4 demonstrates DNA molecule encapsulation into a carbon nanotube performed by the operator through force feedback interface. As the nanotube-DNA interaction experience strong attractive force at near distance (few nanometers), the operator feels unstable insertion forces and guides haptically the molecule along the nanotube.

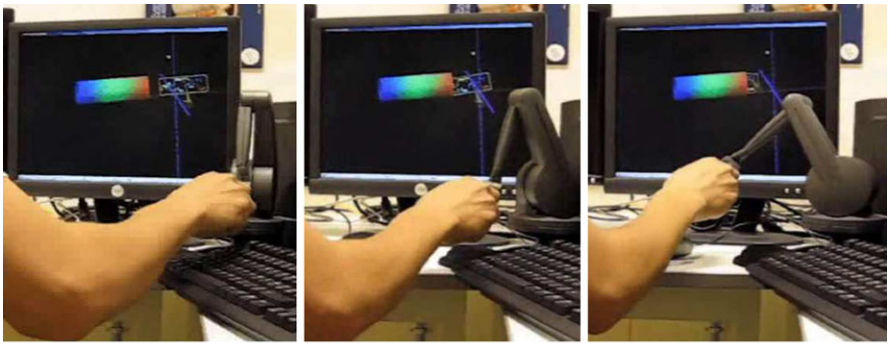


Fig. 2.4 DNA encapsulation in the carbon nanotube using operator force feedback

Tracking System and Input Devices

Virtual Environments (VE) offer a new potential by a more intensive experience of 3D spatial information and natural forms of interaction, to increase the understanding of dynamic spatial relationships. This intensive exposure of scientists to simulation models and data is achieved by representing these as 3D artificial worlds that are suitable for navigation, interaction, and quantification. Intuitive and natural interactions are key aspects of virtual nanoassembly applications.

Intuitive virtual hand interactions with parts, subassemblies and tools is provided by a CyberGlove dataglove (Ascension Technologies CyberGlove18 interface). The 18-sensor data glove features two bend sensors on each finger, four abduction sensors, plus sensors measuring thumb crossover, palm arch, wrist flexion, and wrist abduction. Connected to a 3D tracking device (tracker sensor mounted close to the wrist), it provide the CyberGlove motion capture data glove system with absolute x, y, z, yaw, pitch, roll position and orientation information. A complete tracking system includes one transmitter, one receiver, a system electronics unit with RS-232 serial port. The dataglove interface allows virtual hand representation for manual selection, manipulation and grasping schemes for virtual nanoassembly tasks. Proper registration and calibration of the tracking system is very important. Registration of the tracking system means that we define a transformation from the original tracker coordinate system to a known world coordinate system. Calibration of the tracking system should minimize the tracking errors. Research work is under investigation in order to define grasping patterns based on the abstraction of various mechanic shapes, kinematics model of virtual hand is built upon the anatomic structure of the human hand to guarantee motion realism, and real-time collision detection scheme is used to identify whether the current finger configuration matches a specific manipulation and grasping pattern. Navigation is provided to the user via uniform motion tracking of head interface with immersive displays (stereo glasses). The headtracker is mounted on a pair of LCD shutter glasses. The tracking system enables dynamic spatial measurements of the tracking sensors. The RWB is equipped with a Polhemus Fastrak system, consisting of a control unit, an electromagnetic field emitter

and one or more tracking sensors. The control unit is connected via a serial port. The system is able to determine both spatial position (XYZ) and orientation (AER: azimuth, elevation, roll) of each of the sensors. This results in a total of six degrees of freedom (6 DOF) per sensor.

Interaction Virtual Environment

The user interface with its interaction methods plays a crucial role in nanorobotic design. A virtual environment provides the user interface for VR applications. By using spatial input devices, the user can interact with this computer-generated 3D Virtual Molecular Dynamics environment. In the design of the user interface of our system we concentrated on the user's tasks in scientific visualization and the specific characteristics of VR on the multiscale modeling tools. The designer can choose the desired organic and non-organic elements from an homemade "library bio-nano components". The library is composed of various organic (peptides, proteins, acids) and non-organic (carbon nanotubes, nanoparticles, polymers). The bio-nano components are accessible via a 3-D graphical user interface developed through the VMD environment (see Fig. 2.5). The attachment phase between the different links, structure or peptides with the CNTs can be initiated through 3D virtual manipulation and stereo visualization. The user performs manually the atomistic connections using the data-glove interface or the force feedback haptic interface.

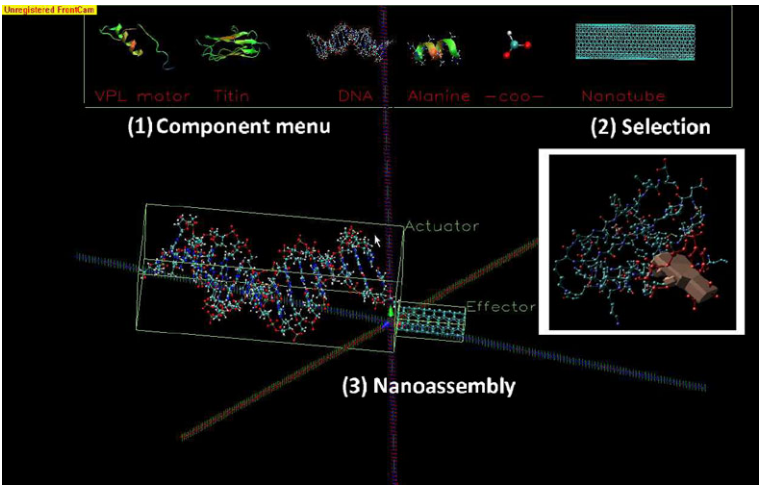


Fig. 2.5 Graphical user interface: bio-nanorobot components are accessible via a 3-D graphical user interface developed through the VMD environment. Illustration task: (*1*) Choice of the components in the library (proteins, biomotors, carbon nanotubes, etc.), (*2*) molecule handling and displacement to a desired location and (*3*) nanoassembly task between a molecule and carbon nanotube

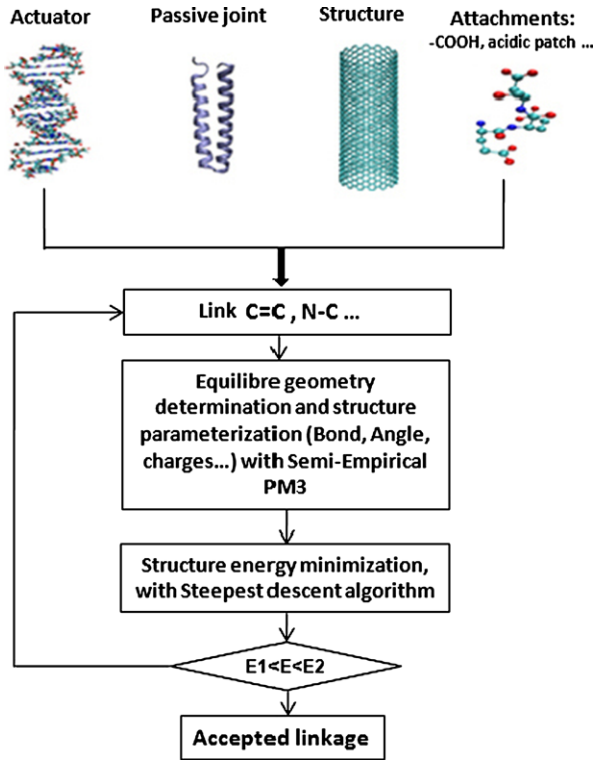


Fig. 2.6 Theoretical and computational nanoassembly methodology

Here we describe the proposed assembly methodology using the described CAD simulation platform. It involves the assembly of functionally stable bio-nano components into complex assemblies. The nanoassembly approach is based on hierarchical theoretical and computational assembly methods depicted on the flowchart shown in Fig. 2.6.

1. The designer can choose the desired organic and non-organic elements from an homemade component database (see Chap. 3). The database is composed of various nanorobotic components such as elastic proteins, carbon structures, protein-based actuators or molecular attachments. The different mechanical, dynamics and kinetics properties of the database structures have been previously characterized. The nanorobotic components are accessible via a 3-D graphical user interface (GUI) developed through the VMD environment.
2. The attachment phase between the different links, structure or proteins can then be initiated through 3D virtual manipulation and stereo visualization. The user performs atomistic connections, i.e. carbon-carbon (C–C), carbon-hydrogen (C–N) bonds in order to create new residues.
3. Such residues are then parameterized through QD simulation in terms of bond length, dihedral angles and Coulomb charges at around the equilibrium state. We use semi-empirical PM3 or Hartree-Fock molecular orbital models with SPARTAN and GAMESS tools.

4. The parameterized attachment is then defined as new residue in CHARMM27 force field. The assembled total nanorobot structure is energetically minimized through the steepest descendent algorithm (SDA) with the respect to two energetic barriers (E1 and E2) corresponding to the energies of acceptable robot geometry.
5. Thus, the program prevents the user from applying the tools in way that is not chemically reasonable.

Multiscale Modeling of Bio-Nano Robotic Structures

Understanding the relation between molecular behavior and system/device response, requires the development of modeling and simulation tools, which can analyze phenomena spanning the wide spectrum of length and time scales. This cannot be accomplished with one theory or simulation method. We have developed a design and modeling platform that dynamically couple all frameworks. We use several physics for particular length- and time-scales to characterize and treat aspects of nanostructure phenomena that operate only over those scales (Fig. 2.7). In the following we present the main characteristics of these methods and how they are combined within multiscale modeling strategies.

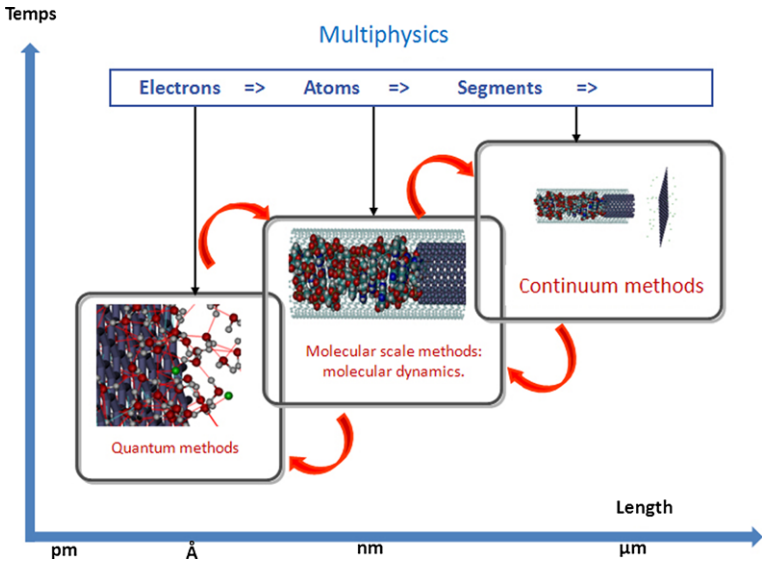


Fig. 2.7 Multiscale modeling of bio-nanorobotics structures

Quantum and Semi-empirical Methods

1. *Quantum Mechanics* (*QM*): A wide variety of different procedures or "models" have been developed to calculate molecular structure and energetics among other properties. Theses have generally been broken down into two categories, quantum chemical models, which ultimately derive from the Schrödinger equation, and molecular mechanics models. In atomic units, the electronic Schrödinger equation is

$$\hat{H}\Psi(r;R) = \varepsilon\Psi(r;R) \tag{2.5}$$

where r and R denotes electronic and nuclear degrees of freedom and $\hat{H}$ denotes the Hamiltonian operator. The term $\hat{H}$ describes both the kinetic energies of the nuclei and electrons which makeup the molecule, as well as the electrostatic interactions felt between the nucleic and electrons. The Hamiltonian is given by

$$\hat{H} = -\frac{1}{2}\sum_i \nabla_i^2 - \sum_{r,i}\frac{Z_A}{r_{Ai}} - \sum_i \frac{Z_A Z_B}{R_{AB}} + \sum_{i>j}\frac{1}{r_{ij}} \tag{2.6}$$

where A and B design nuclei, and i and j electrons, Z are the atomic numbers, and atomic units are used in (2.5).

2. *Hartree-Fock Molecular Orbital Models*: Although the Schrödinger equation may easily be written down for many electron atoms as well as for molecules, it cannot be solved. Approximation must be made. So called Hartree-Fock molecular orbital models [30], start from the Schrodinger equation and then make three approximations: (i) separation of nuclear and electron motions (the "Born-Oppenheimer approximation"), (ii) separation of electrons motions (the "Hartree-Fock approximation") and (iii) representation of the individual molecular orbital in terms of linear combinations of atom-centered basis function or "atomic orbitals".

   The Hartree-Fock approximation is an extension of the above Hartree approximation to include the permutation symmetry of the wavefunction which leads to the exchange interaction. Exchange is due to the Pauli exclusion principle, which states that the total wavefunction for the system must be antisymmetric under particle exchange. This means that when two arguments are swapped the wavefunction changes sign as follows:

$$\Psi(x_1, x_2, \ldots, x_i, x_j, \ldots, x_N) = -\Psi(x_1, x_2, \ldots, x_j, \ldots, x_N)$$

where x_i includes coordinates of position and spin. Therefore no two electrons can have the same set of quantum numbers, and electrons with the same spin cannot occupy the same state simultaneously. Instead of using a simple product form of the wavefunction, a Slater determinant wavefunction which satisfies

antisymmetry is used. This can be represented in matrix notation as

$$D = \begin{vmatrix} \psi_1(1) & \psi_2(1) & \psi_3(1) & \cdots & \psi_n(1) \\ \psi_1(2) & \psi_1(2) & \psi_1(2) & \cdots & \psi_n(2) \\ \cdots & \cdots & \cdots & \cdots & \cdots \\ \psi_1(n) & \psi_2(n) & \psi_3(n) & \cdots & \psi_n(n) \end{vmatrix} \tag{2.7}$$

where $\psi_i(x_j)$ are the one-electron wavefunctions.

Following exactly the same method of minimizing the expectation value of the Hamiltonian $\hat{H}$ with respect to the one-electron wavefunctions as was used in the derivation of the Hartree equations, results in the following set of one-electron equations, the Hartree-Fock equations;

$$\epsilon_i \psi_i(r) = \left(-\frac{1}{2}\nabla^2 + U_{ion}(r)\right)\psi_i(r) + \sum_j \int dr' \frac{|\psi_j(r')|^2}{|r - r'|}\psi_j(r)$$

$$- \sum_j \delta_{s_i s_j} \int dr' \frac{\psi_j^*(r')\psi_i(r')}{|r - r'|}\psi_j(r)$$

where s_i labels the spin of particle i.

3. *Semi-Empirical Molecular Orbital Models*: The principal disadvantage of Hartree-Fock models is their cost [31]. It is possible to introduce further approximations in order to significantly reduce cost while still retaining the underlying quantum mechanical formalism. "Semi-empirical" molecular orbital models follow in a straightforward way from Hartree-Fock models: elimination of overlap between functions on different atoms, restriction to a "minimal valence basis set" of atomic functions and introduction of adjustable parameters to reproduce specific experimental data. The Stewart's Parametric Method Number 3 (PM3) semi-empirical model is particularly attractive for equilibrium and transition-state geometry determinations for large molecules where the costs of Hartree-Fock models may be prohibitive.
4. *Molecular Mechanics Models*: The alternative to quantum chemical models are molecular mechanics models [32]. These do not start from the Schrödinger equation, but rather from a simple but "chemically reasonable" picture of molecular structure, a so-called "force field". In this picture, just as with a Lewis structure, molecules are made up of atoms (as opposed to nuclei and electrons), some of which are connected ("Bonded"). Both crowding ("Van der Waals") and charges ("Coulombic") interactions between atoms are then considered, and atom position are adjusted to best match known structural data (bond lengths and angles). Molecular mechanics is much simpler than solving the Schrödinger equation.

   The PM3 semi-empirical model is suitable for identifying conformational minima, and for determining the geometries (bond lengths, angles and charges) of these minima.
5. *Semi-empirical Parameter Generation*: When attaching a residue termini to another one, such for example attaching leucine termini to graphite layer, a novel

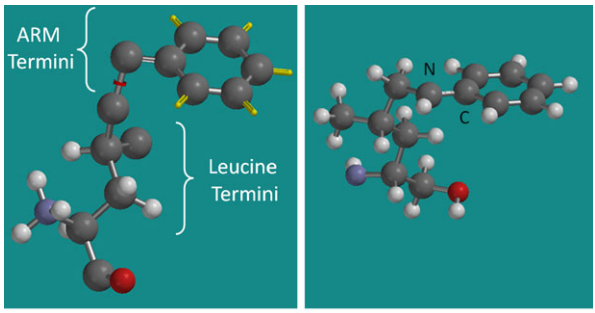


Fig. 2.8 (**a**) Leucine-ARM residues linkage and (**b**) linkage equilibrium geometry at ground state with Semi-Empirical PM3

nonstandard group become created (see Fig. 2.8(a)), the first task is to determine exactly which parameters are already known, and which will need to be developed from scratch. The unparameterized part of the new residue is the connection between the azote and the carbon. The connection between the azote of LEU and the carbonyl carbon of the ARM residue is called a thioester bond. Leucine-ARM linkage is defined as a new residue defined as a new residue in the CHARMM27 topology [33] file with the name LARM. In order to use this LARM residue in MD simulations, we need to make a topology file entry for it as well as develop a complete set of parameters describing it. The unparameterized part of the LARM residue is the connection between the leucine and the carbon.

To actually determine the optimum parameter values for equilibrium bond lengths, angles, and to determine the energetic barriers associated with them, we need to use quantum chemistry. For our study, we use SPARTAN to generate these values. We calculate the values semi-empirically. With semi-empirical quantum mechanics calculation, we optimize the geometry of the structure as shown in Fig. 3.16(b), calculate electrostatic potential (ESP) charges and vibrational frequencies. The LARM linkage, which correspond to C–N bond, calculated by SPARTAN semi-empirical PM3 methods is 1.449 Å and C–N–C angle is 123.25°. The LARM linkage parameters (angles, bonds lengths, charges) will be add to CHARMM27 force field to be used in molecular dynamics level.

Molecular Dynamics

We carry out computer simulations in the hope of understanding the properties of assemblies of molecules in terms of their structure and the microscopic interactions between them. This serves as a complement to conventional experiments, enabling us to learn something new, something that cannot be found out in other ways. The two main families of simulation technique are molecular dynamics (MD) and Monte Carlo (MC) [33]; additionally, there is a whole range of hybrid techniques which combine features from both. In this lecture we shall concentrate on MD. The obvious advantage of MD over MC is that it gives a route to dynamical properties of the

system: transport coefficients, time-dependent responses to perturbations, rheological properties and spectra.

To predict the dynamic performance of a designed nanodevice (i.e., energy and force calculation), we are performing Molecular Dynamics (MD) Simulations based on the calculation of the free energy that is released during the transition from native to fusogenic state. We used MD software called NAMD (Chemistry at Harvard Molecular Mechanics) [15]. In MD, the feasibility of a particular conformation of the biomolecule in question is dictated by the energy constraints. Hence, a transition from one given state to another must be energetically favorable, unless there is an external impetus that helps the molecule overcome the energy barrier. When a macromolecule changes conformation, the interactions of its individual atoms with each other-as well as with the solvent compose a very complex force system. The NAMD energy function is given:

$$U(\overrightarrow{r1}, \overrightarrow{r2}, \ldots, \overrightarrow{r_N}) = U(\overrightarrow{R}). \tag{2.8}$$

The equation used to determine the force on each atom as:

$$m_i \frac{d^2 \overrightarrow{ri}}{dt^2} = \overrightarrow{F_i} = -\overrightarrow{\nabla} U(\overrightarrow{R}). \tag{2.9}$$

Newton's equation represents a set of N second order differential equations which are solved numerically at discrete time steps to determine the trajectory of each atom.

$$\overrightarrow{r_i}(t + \Delta t) = 2\overrightarrow{r_i}(t) - \overrightarrow{r_i}(t - \Delta t) + \frac{\Delta t^2}{m_i} \overrightarrow{F_i}(t). \tag{2.10}$$

The total energy is given by:

$$U(\overrightarrow{R}) = U_b + U_\theta + U_\omega + E_{vdw} + E_{elec}. \tag{2.11}$$

The individual components of the total energy U are the bond potential U_b, the bond angle potential U_θ, the dihedral angle potential U_ω, the Van der Waals Potential U_{vdw}, the electrostatic potential function U_{elec}. The functional forms of these potentials are as follows: Bond potential is given by

$$U_b = \sum_{bonds} k_i^{bond} (r_i - r_0)^2.$$

The variable r is an instantaneous bond length due to an extension or contraction of a bond and r_0 is its original length. Similarly, the bond angle potential is given by

$$U_\theta = \sum_{angles} k_i^{angle} (\theta_i - \theta_0)^2. \tag{2.12}$$

Angle θ is the deviation from the equilibrium value θ of the bond angle for a given set of atoms. Under normal temperature conditions, these two potential values are

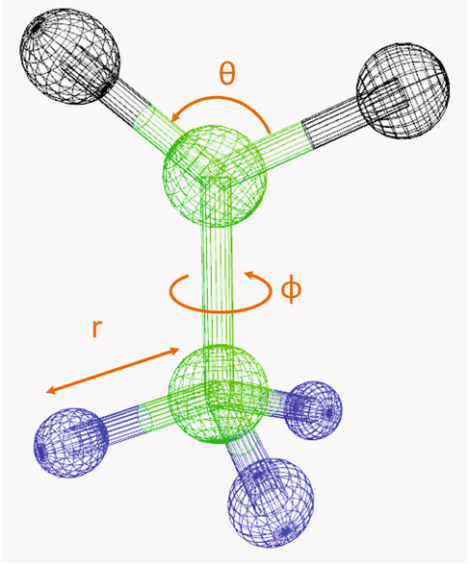


Fig. 2.9 Internal coordinates for bonded interactions: r governs bond stretching; θ represents the bond angle term; ϕ gives the dihedral angle

very small, as the bond lengths and angles do not change appreciably. However, there is rotation around certain bonds (torsion or bond twist). The dihedral angle or torsion potential is thus formulated, which is given by

$$U_{\omega} = \sum_{dihedrals} k_i^{dihe}[1 + \cos(n_i\phi_i + \delta_i)]. \tag{2.13}$$

This term is a four-atom term based on the dihedral angle ϕ about an axis defined by the middle pair of atoms. The electrodynamic effect of Van der Waals forces is included by using the Lennard-Jones potential as:

$$U_{vdw} = \sum_i \sum_{j \neq i} 4\epsilon_{ij}\left[\left(\frac{\sigma_{ij}}{r_{ij}}\right)^{12} - \left(\frac{\sigma_{ij}}{r_{ij}}\right)^{6}\right]. \tag{2.14}$$

In the above equation, ϵ_{ij} represents the energy of the minimum (deepest) point on Van der Waals curve for the atom pair $i - j$, σ_{ij} is the separation distance between the atom pair $i - j$ at the energy minima, and r_{ij} is the current actual distance between atom i and atom j. The attractive forces between two proximal atoms are proportional to r_{ij}^{-6} and the repulsive forces due to their nuclear repulsions are proportional to r_{ij}^{-12}. The other important factor in nonbonded interaction is the electrostatic interaction, which for atoms i and j, is given by:

$$U_{elec} = \sum_i \sum_{j \neq i} \frac{q_i q_j}{\epsilon r_{ij}}. \tag{2.15}$$

Combined Molecular Dynamics and Continuum Approach

The main goal of molecular dynamics studies is to understand the relation between molecular behavior and nanorobot response. Molecular dynamics computing time may take a very long time, thus evaluation of the controller design can not be achieved through realtime simulation. Some nanorobot elements, such as Immunoglobulin, DNA and Fibronectin has been described as a molecule that acts like a molecular spring and different corresponding models can be adopted. To overcome the long time computing problem, the proteins spring was modeled by the Worm Like Chain (WLC) or Hookian model in molecular dynamics. The Hookian and WLC model was implemented as TCL script, and communicate in realtime with NAMD program during simulations. In order to compare the performances of quantum mechanics-molecular dynamics (QM-MD) and quantum mechanics-molecular dynamics-continuum mechanics (QM-MD-CM), we performed several calculations. It can be noticed that for acceptable results of simulation, the QM-MD-CM reduces the complexity of nanorobotic structures (decrease of number of atoms) to be simulated for smaller computational time (around few milliseconds) and smaller simulation times (nanosecond order), those results will be detailed in the next chapter. We adopt WLC model for passive joints-based proteins Fibronectin Fn-III$_{10}$, Immunoglobulin I27, Tropocollagen, silk, DNA and Tropomyosin, that describes a molecular chain as deformable continuum or rod of given persistance length, A, which is a measure of the molecule's stiffness. The relationship between the end-to-end length (z) and the external force (f) are given by:

$$f = \frac{KT}{A}\left[\frac{1}{4(1-\frac{Z}{L})^2} - \frac{1}{4} + \frac{z}{L}\right] \tag{2.16}$$

where k is the Boltzman constant, T is the temperature, and L is contour length (the length of fully extended WLC chain). For our simulations the persistence length is settled to $A = 0.4$ nm (see [35]). In order to determine the value of the protein length L, we summed the contour lengths of all the protein domains when considered in its fully extended state. It results that the contour length is proportional to the number of amino acids [36]. The corresponding external force increases linearly as a Hookes for α-helix deca-alanine, repressor of primer protein and fibrillin protein. The extension of the Hookian spring is proportional to the force applied at its end such as:

$$f = \left(\frac{k_B T}{A}\right)\left(\frac{x}{L}\right). \tag{2.17}$$

Mechanical Characterization by Steered Molecular Dynamics

Biological springs can be classified as active mechano-chemical devices that store the energy of conformation from various bonded and non-bonded interactions as potential energy. To characterize the mechanochemical energy conversion and to study

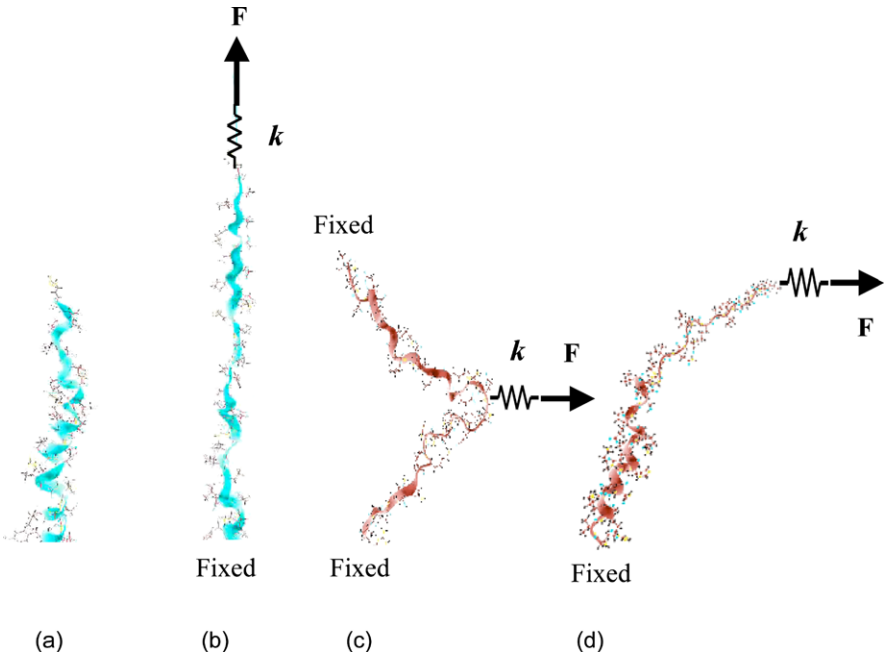


Fig. 2.10 Schematic diagrams of the various deformations studied with the attachment points used for mechanical unfolding experiments. *The arrows* indicate the positions where the stretching constraints were applied and the direction of stretching. (**a**) Folded configuration of helical protein, (**b**) longitudinal stretching, (**c**) lateral bending and (**d**) lateral shearing. The moving guiding potential used in the stretching simulations is represented by a spring k which is pulled with a constant velocity v

the elasto-mechanical properties of these biological springs external are applied using steered molecular dynamics. To study some mechanical proprieties various deformations properties of mechanical proteins can be simulated when subjected to external stretching. First, (i) in longitudinal stretching (Fig. 2.10(b)), we fix one end of the molecule (the C-atom of the N-terminus) at the origin and constrain the other end (the capping nitrogen atom of the C-terminus) to move only along the longitudinal axis, thereby removing the irrelevant degrees of freedom, i.e., removing the overall translation and rotation. Then, (ii) in lateral bending (Fig. 2.10(c)), the C- and N-terminals are fixed and the α carbon at the center is harmonically pulled in lateral direction. Finally, (iii) in lateral shearing (Fig. 2.10(d)), the C-terminal is held fixed and the N-terminal is harmonically pulled in lateral direction. The moving guiding potential:

$$u(r, \lambda) = \frac{k}{2}[\xi(r) - \lambda]^2 \tag{2.18}$$

is added to control the end-to-end distance x which is a function of the 3N-dimensional position r of the system. The moving guiding potential used in the pulling simulations is represented by a spring which is connected to the C-terminus and

pulled with a constant velocity v. For each protein, the values of the spring constant k and stretching velocity v were chosen to correspond pulling with a stiff spring in the drift regime. the external force exerted on the system can be expressed as

$$F = K(x_0 + vt - x). \tag{2.19}$$

This force corresponds to the ligand being pulled by a harmonic spring of stiffness K with its end moving with velocity v. Alternatively, a fixed restraint point at a distance much larger than the length of the unbinding pathway may be chosen. In this case, the end of the spring does not move and its stiffness is linearly increased with time [37], i.e., $K = \alpha t$, and the force is

$$F = \alpha t(x_0 - x). \tag{2.20}$$

Control Parameters Coupled to Molecular Dynamics

pH Control

Numerous protein-based nanodevices show a spontaneous "opening" and "closing" mechanism upon temperature, pH, light, ionic strength and electron density modulation and can be considered as a basic molecular motor, nanogripper or nanosensor capable of generating mechanical force during its 3D conformational transition. These control parameters have been included in the molecular dynamics algorithms in order to prototype controlled mechanical motion. As illustration, Fig. 2.11 shows the conformation control of a viral protein motor (VPL) when considering the pH variation. It changes the energetics of the outer (envelope glycoprotein) protein in such a way that there is a distinct conformational change in a part of it. Proteins

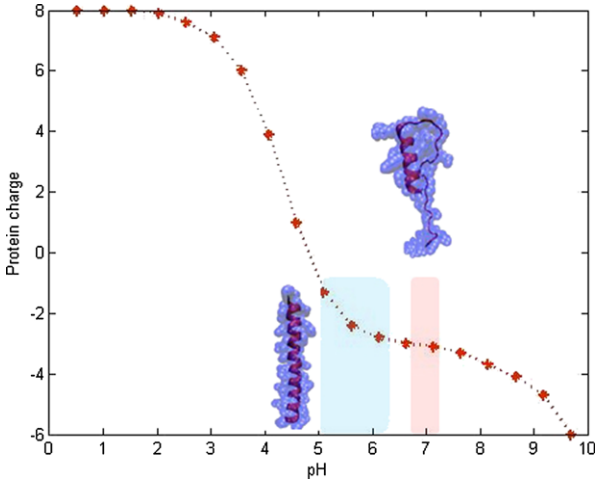


Fig. 2.11 Charge on amino acids side chains in viral protein with respect to the level of pH

contain many ionizable groups on the side chain of their amino acids. pH is the negative log of the hydrogen ion concentration in a solution such as $pH = -\log[H^+]$. For a neutral acidic pH value ($pH = 7$), the VPL protein is in a partially α-helical stranded coiled coil. The random coil regions are converted into well defined helices and an extension occurs at lower pH between 5 and 6.5. For this configuration, it is necessary to protonate the amino acid side chain of the protein. Because Molecular dynamics simulations are used to simulate the motion of molecules in order to gain a deeper understanding of the chemical reactions, fluid flow, phase transitions, and other physical phenomena due to molecular interactions. Rapidly increasing computational power has made MD simulation a powerful tool for studying the structure and dynamics of biologically important molecules. Taking into account all electrostatic interactions by using the Particle Mesh Ewald (PME) method, relatively long (2–3 ns) simulations with the explicit solvent water box can be carried out. We perform constant-pH molecular dynamics (MD) simulations with an implicit solvent and explicit treatment of protonation/deprotonation phenomena. The protonation state of each ionizable group in the molecule is allowed to change during the MD trajectory at predefined time intervals, dividing the whole simulation into a set of sub-trajectories. Each change in the protonation state of the molecule at the beginning of a new sub-trajectory is made with a probability determined by the electrostatic free energies of the available states, based on the last structure of the preceding sub-trajectory.

In Chap. 3, the influence of these control parameters will be discussed in detail through the MD study of different bio-nano components. As experimental evaluation for such optimum conditions is very time consuming and costly, computer-aided modeling and simulation studies are helpful to identify the optimum control parameters in an effective way.

Thermal Control of Nanodevices

The strong sensitivity of the force-extension characteristics of the DNA molecule and elastic joint proteins to temperature plays an important role in the control of their stiffness [21]. Indeed, the overstretching portions of the force-extension curves as a function of temperature decrease greatly as the temperature is increased. As example, [56] shows the evolution of the DNA spring constant K_{DNA} with respect to the temperature ranging from 273 to 450 K. In theory, the results show clearly the linear decrease of spring constant with respect to the temperature. Constant temperature molecular dynamics simulations are used to simulate the effect of temperature in the mechanical characteristics of biological elastic joint. Constant temperature control during simulation is performed by the use of canonical ensemble *NVT* where, moles (N), volume (V) and temperature (T) are conserved. NAMD use a stochastic coupling approach because it is easier to implement and the friction terms tend to enhance the dynamical stability. The Langevin equation is used in NAMD to generate the Boltzmann distribution for canonical (*NVT*) ensemble simulations. The

generic Langevin equation is

$$M\dot{v} = F(r) - \gamma v + \sqrt{\frac{2\gamma k_B T}{M}} R(t) \tag{2.21}$$

where M is the mass, $v = \dot{r}$ is the velocity, F is the force, r is the position, γ is the friction coefficient, k_B is the Boltzmann constant, T is the temperature, and $R(t)$ is a univariate Gaussian random process. Coupling to the reservoir is modeled by adding the fluctuating (the last term) and dissipitive ($-\gamma v$ term) forces to the Newtonian equations of the motion. To integrate the Langevin equation, NAMD uses the Brüger-Brooks-Karplus (BBK) method, a naturel extension of the Verlet method for the Langevin equation. The position recurrence relation of the BBK method is

$$\begin{aligned} r_{n+1} = r_n + \frac{1 - \gamma \Delta t/2}{1 + \gamma \Delta t/2}(r_n - rn + 1) \\ + \frac{1}{1 + \gamma \Delta t/2} \Delta t^2 \left[M^{-1} F(r_n) + \sqrt{\frac{2\gamma k_B T}{\Delta M}} Z_n \right] \end{aligned} \tag{2.22}$$

where Z_n is a set of Gaussian random variables of zero mean and variance 1. The BBK integrator requires only one random number for each degree of freedom. The steady-state distribution generated by the BBK method has an error proportional to Δt^2, although the error in the time correlation function can have an error proportional to Δt.

3 Co-prototyping of Nanorobotic Structures

Carbon Nanotubes Based Nanodevice Co-prototyping

Generally, prototyping of nanorobotic devices and structures may be impractical due to very high cost or low performance requirements. Much of the costs of today's processes are the result of meticulous design prior to fabrication and extensive testing (e.g. defect detection) after fabrication. A solution would be to use hardware and software co-design methodologies focusing on the prediction of system performance or co-verification of system functionality Fig. 2.12, the design stage is subdivided into two main parallel steps (namely, computational simulation and experimentation) leading to the nanodevice prototyping stage. As molecular simulations allow running several nanodevice tests within a theoretical model, we can update this computational model from real nanodevice experimentation leading to realistic and low-cost testing and prototyping.

As illustration of this concept, we developed a co-prototyping methodology applicable to various multiwalled carbon nanostructures. Figure 2.13 outlines the main steps ranging from basic design specifications to optimized prototyping of the

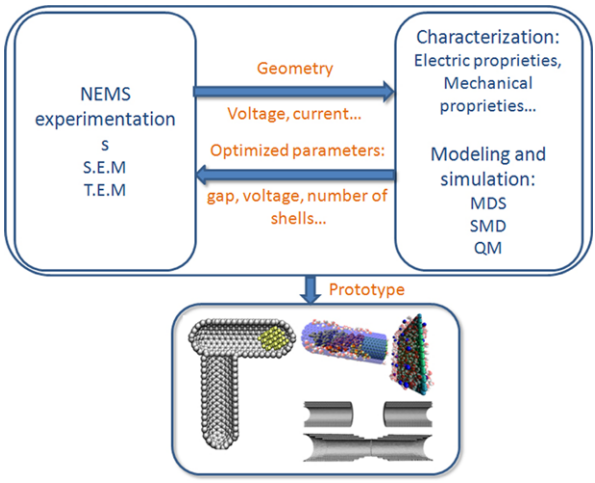


Fig. 2.12 Co-design and co-prototyping of based carbon nanotubes nanodevices

nanosystem. The first step in is the design of the nanosystem model by coupling theoretical data to carbon nanotube experimental measures.

The second phase, presents the nanodevice co-prototyping. The study and the characterization of the nanodevice is performed mainly by simulations based on realistic models. The model of the structure is updated interactively from the experimental. Simulations allow mainly three functions: characterize and explain the nanodevice behavior, to optimize the nanodevice (such as the determination of the configuration which correspond to a minimum of consumed electric potential) and finally to observe specific phenomena, which are not observable by experimentations (such as the rotation of the inner carbon nanotubes), this can be helpful for the design of the new nanodevices.

After the prototype has been validated, it is all prepared for the serial fabrication of the prototype.

Figure 2.1 illustrates the outline of co-prototyping method. In the proposed co-prototyping methodology, the prototype was intuitively designed in the above step as described by Fig. 2.13. Prototyping of the proposed nanodevice require several repetitive experimental tasks, because the hight cost of these kind of manipulation we use theoretical approaches to performs specific prototyping tasks. Prototyping flow begins with specification of designed system, by gathering the proprieties of the system from experimental platform, mainly from experimentation we consider the device dimension and the control parameters such as the actuation voltage. Prototyping the nanodevice by using simulations require system characterization and modeling. The designed system is characterized, electric proprieties are carried out, by using Quantum methods and atomistic moment method we calculate the charge redistribution along the nanodevice. We perform molecular dynamics simulations (MDS) to study the system characterization. As initial model used in MDS we generate the 3D system coordinate (xyz) by using dimensions gathered from experimentation. The we perform molecular dynamics simulation to characterize specific proprieties of the proposed system, such as the optimal actuation voltage consid-

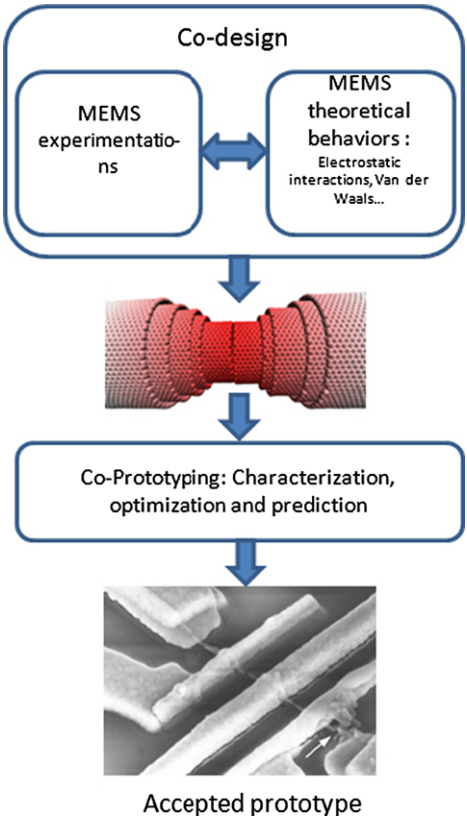


Fig. 2.13 Co-design of carbon nanotube based nanodevice

ering the number of shells in a based multiwalled carbon nanotube devices. The optimal actuation voltage for different configuration.

Simulation Methods

The methods of modeling the atomic interactions can roughly be divided into three categories: The first principles, or *ab-initio*, methods are the most rigorous ones. Only a few well controlled approximations to exact quantum mechanics are made. Semi-empirical methods contain more drastic approximations and may also contain empirically defined parameters. Empirical methods are a group of methods that are tuned to reproduce an empirically defined fitting set. The three categories, their drawbacks and benefits, and the most popular methods of each are briefly described in this section. The most rigorous approach to problems of condensed matter physics are the first principles methods. They do not employ any empirical parameters in the calculation. The results are based on quantum mechanics and well controlled approximations. The two most used first principles methods are the Hartree-Fock

method and the density functional theory [38, 39]. The first principles methods are highly accurate but the system size that can be handled is restricted to tens, at most a couple of hundred atoms. The Hartree approach to the quantum mechanical many body wave function is to approximate the function by a product of single particle functions. The approximation is refined by adding Fermi-Dirac statistics by replacing the product of the wave functions by the Slater determinant. The method obtained with this inclusion is called the Hartree-Fock approach [30]. Even though the method is not always extremely accurate, it is much used. The accuracy can be enhanced but this increases the consumption of CPU-time [40]. In its most rigorous form,the Hartree-Fock method can be used on systems of tens of atoms. Density Functional Theory (DFT) [38, 39] is based on using the electron density $n(\overrightarrow{r})$ of the system as the basic variable. The ground state is completely described by the electron density as stated by the Kohn-Sham theorem [38, 39]. There are various schemes of determining the energy of the system from the electron density. In the most simple form of DFT, in local density approximation (LDA), the expressions based on a non-interacting electron gas at the local electron density of the real system. Currently DFT is a very accurate method and its accuracy can be enhanced by the use of methods combining Hartree-Fock and DFT description, for example, B3LYP1 functional description [40]. DFT can be used on systems of a few hundred atoms.

Semi-empirical Methods

Semi-empirical methods employ various approximations and may include experimentally fitted parameters. Their power with respect to the first principles methods lies in a smaller consumption of CPU-time but they must be employed more carefully to obtain reliable results. Semi-empirical methods include interaction schemes like the tight binding method (TB) [41] and various molecular orbital methods of computational chemistry [40]. The tight binding method avoids most of the heavy calculation of the *ab-initio* methods. There are several methods in this family. The TB-methods have in common a number of simplifications such as minimal basis sets compared to the first-principles methods and elimination of difficult integrals, that are either made small by mathematical transformations or used as parameters to be fit to experimental data. In principle, everything that can be calculated by the *ab-initio* methods can be calculated by an appropriate tight binding method and with less CPU-time. The keyword above is the 'appropriate': the generality and the transferability of a tight binding method depend on the approximations. Although valid for thousands of particles, the method used must be assessed case-specifically. In computational chemistry the methods similar to tight binding are called the neglect of diatomic differential overlap methods [40]. Also these methods simplify the involved integrals but retain the molecular orbital description. The group involves various methods such as AM12 and PM33 [40].

Empirical Methods

The category of empirical methods contains a wide set of parameterized classical force fields that reproduce more or less accurately the fitting set that is determined either from experimental data or from *ab-initio* simulations. Force-field methods have the benefit of being computationally simple and thus fast. They allow the simulation of large systems (up to hundreds of millions of atoms) over a greater time-span (up to microseconds) than the methods presented above. The simplest approximation for the interaction potential takes into account only two-particle interactions. Potentials like this are called pair potentials. The Lennard-Jones potential [42] and the Morse potential [43] are two very well known examples of pair potentials. Although pair potentials are not ideal for the study of the mechanical properties of materials, they are very much used because they are simple to implement and algorithms based on pair potentials are kind on computational resources. There are, however, some severe shortcomings which should be taken into account whenever pair potentials are used. For example, an interaction described by a pair potential model can depend only on the distance between the two particles. Thus the potential can not model directional bonding. Pair potentials often predict wrong vacancy formation energies and melting temperatures [42, 43]. The construction of an accurate force-field encounters often system and material based difficulties, and often even fundamental limitations. Difficult media are metals, alloys, semiconductors, and oxide-based insulators. In this thesis the emphasis is, of course, on carbon. Describing carbon accurately requires a lot of caution and is difficult because the 2s electrons participate in molecular bonding and together with the 2p electron orbitals hybridize to form a wide variety of potential bonding configurations that depend on the environment and on the ambient conditions. Even by itself, carbon can form structures as diverse as the isotropic diamond crystal or the anisotropic planar graphite and nanostructures. If the consideration is extended to organic molecules, even only hydrocarbons, the bonding variety, and at the same time the complexity of describing it accurately, becomes vast. If covalently bonding materials, like sp2-carbon, are simulated, the modeling of directional bonding is essential in order not to obtain outright wrong results. In general this means that the interaction potential used must include at least a three-body interaction term. Because carbon is the basis of all organic materials and because diamond and graphite have various applications in materials science, numerous attempts to create accurate classical interaction potentials have been made but only a few of the proposed schemes are widespread. For example, carbon interaction potentials developed by Tersoff in [44–46] and Brenner in [47] are widely used in the modeling of carbon. The Brenner model is considered more versatile because of additional conjugated bond description while the structures modeled by the Tersoff model suffer from an overbinding of radicals and the description of systems involving bonds that exhibit a mixture of sp3 and sp2 hybridization is inaccurate. Both models are short ranged and cover only the nearest neighbors to speed up the calculations. For description of graphite or multi-walled nanotubes, much longer range interactions are required. Various long-range extensions that are most often based on Lennard-Jones type additional term to describe

the ∂-bonding have been proposed. Stuart et al. [48] have aimed at maintaining the reactivity description of the Brenner [47] model while introducing the long-range interactions. Therefore, this model was chosen where long-range interactions are required. In general the force-field methods can give information on the structure and dynamics of a system, the total energies, entropies, free energies, and diffusive processes in the system. By their construction the methods are incapable of predicting any properties related to the electronic structure such as electrical conductivity, optical, or magnetic properties. In short, the classical force field methods are structural tools. The general accuracy of results obtained by classical force field methods is far from the level of accuracy obtained by *ab-initio* simulations but so are the feasible system size and attainable time scale as well.

In this work the emphasis is on studying carbon nanotube properties through classical means. The choice allows studying structures that have dimensions comparable to the experimentally observed ones. Classical molecular dynamics with AIREBO potential [48] are employed in the simulation. The potential used for this work is based on the reactive empirical bond-order potential of Brenner.

The reactive empirical bond-order (REBO) model is a widely-used theory to calculate the potential energy of covalent bonds. In 1988, based on works of Abell [49], Tersoff proposed a many-body energy function [44] parameterized for carbon [45] and multicomponent systems [46]. The expression of the total potential energy of system is a sum of nearest-neighbour pair interactions which depend not only on the coordination of atoms but also on their local atomic environment. A simple parameterized bond order function was used to describe chemical pair bonded interactions. This theory could realistically describe single, double and triple bond energies of carbon structures such as some hydrocarbons and diamond. A significant step was taken by Brenner for conjugated hydrocarbons and carbon system in 1990. He extended Tersoff's potential function by introducing two additional terms into the bond order to describe radical and conjugated bonds.

Because only nearest-neighbour interactions have been considered, the REBO function could be quickly evaluated. This computational efficiency could therefore be well adapted in numeric simulations [50]. In the research works concerning the mechanical properties of carbon nanotubes in past 20 years, REBO functions have been used to study the elastic properties [51] and the structural stabilities (defect, buckling, ultimate strength and bond breaking, ...) [52] of CNTs. An acceptable accuracy has been reported in some of these works, by comparing with the experimental, ab initio or tightbinding results. Despite numerous successful applications of the first-generation REBO potential functions, they suffer from several drawbacks. First, its form is too restrictive to simultaneously fit equilibrium distances, energies, and force constants for all types of carbon-carbon bonds. Second, the possibility of modeling processes involving energetic atomic collisions is limited because both Morse-type terms go to finite values as the distance between atoms decreases. Third, the absence of dispersion and the non-bonded repulsion term make the potential poorly suited for any system with significant intermolecular interaction. In the simulation of carbon nanotubes under bending strain, the REBO potential has been reported to lead direct inaccuracy at high level of deformation [53]. Finally, it has

been reported by Pettifor and co-workers [54] that the neglect of a separate ∂ bond contribution leads to problems with the overbinding of radicals and a poor treatment of conjugacy. So as to resolve these problems, an adaptive intermolecular reactive bond order (AIREBO) function has been proposed by Stuart and co-workers [48] in 2000. In this theory, the entire system energy was given by the expression

$$U^p = U^{REBO} + U^{non\text{-}bonded} + U^{single\text{-}bond\text{-}torsion} \tag{2.23}$$

$U^{non\text{-}bonded}$ is the non-bonded interactions term (Lennard-Jones 12-6 potential function), and $E^{single\text{-}bond\text{-}torsion}$ represents the torsional interactions about single bonds. Both the repulsive and the attractive pair interaction functions have been modified to simultaneously fit bond properties that could not be fitted by the first-generation Brenner's function. This potential function can be well adapted to reactive systems.

In the REBO potential, the chemical binding energy U_b is a collection of that of individual atoms, in which only the nearest-neighbour interactions are considered.

$$U_b = \sum_{i=1}^{N} \sum_{\substack{j=1 \\ i=1}}^{N} \left[V^R(r_{i,j}) - b_{i,j} V^A(r_{i,j}) \right] \tag{2.24}$$

where $\varphi^R(r_{i,j})$ and $\varphi^A(r_{i,j})$ are the interatomic repulsion and attraction terms, r_{ij} is the distance between atoms i and j and b_{ij} is the bond order function between atoms i and j that is derived from Huckel electronic structure theory. All many-body effects are included in this function.

In the AIREBO potential, the dispersion and intermolecular repulsion interactions are modeled with a Lennard-Jones 12-6 potential function

$$U_{LJ} = 4\epsilon \left[\left(\frac{\sigma_{ij}}{r_{ji}} \right)^{12} - \left(\frac{\sigma_{ij}}{r_{ji}} \right)^{6} \right]. \tag{2.25}$$

The other new component of the AIREBO potential is a term dependent on dihedral angles. The original REBO potential lacked any torsional interactions about single bonds, reflecting its original focus on network solids such as diamond and small molecular fragments relevant to the chemical vapor deposition of diamond. With no barrier to rotation about single bonds, however, the original REBO potential is poorly suited for the simulation of saturated hydrocarbons larger than methane. As with the nonbonded interactions, the reactive nature of the potential requires some modifications to the conventional method of introducing torsional interactions. The usual form for the torsional potential is a cosine power series in the dihedral angle ω.

The total potential energy of system is

$$U^{tot} = U^{elec} + U^P \tag{2.26}$$

where U^{elec} is the electrostatic energy due to the extra charges on two carbon atoms and U^p is the AIREBO interatomic potential. The electrostatic energy can be calculated by the coulomb law: $E_{ij}^q = \frac{q_i q_j}{4\pi\varepsilon R_{ij}}$, where q_i and q_j are extra charges on carbon atoms, R_{ij} is the interatomic distance, and ε is the permittivity.

The charge distribution on the carbon nanotube is obtained by an atomistic moment method based on classical electrostatics theory [55]. In our simulations, we consider a multi walled carbon nanotube (MWCNT) with finite length. For simplicity, the nanotube is assumed to be located in an idealized electric field, i.e., the voltage on the on the nanotube surface is V_0. If we consider a carbon nanotube with n atoms, the potential at an arbitrary atomic position is given by [55]:

$$V(r_i) = \sum_{j=i}^{n} \frac{q_j}{4\pi\varepsilon_0 |r_i - r_j|} \tag{2.27}$$

where V is the electric potential, q_j the point charge on the atoms, r_i represents the location of the charged atom, and ε_0 is the permittivity of vacuum. Because the equipotential status of the nanotube surface, n equations can be written in a matrix form, i.e.,

$$[A]\{q\} = V \tag{2.28}$$

where $\{q\}$, V are the charge vector and the potential vector, respectively, and $[A]$ is the $n * n$ order matrix. Equation (2.28) is no longer applicable. For calculating the diagonal terms of the coefficient matrix, we need to recall the original assumption that the charge is uniformly distributed on a triangular surface area surrounding the carbon atom, as shown in Fig. 2.14. For simplicity, we treat the actual three-dimensional curve surface approximately as a flat triangle. The area of the triangle is $s = \frac{3\sqrt{3}b^2}{4}$, where $b = 0.142$ nm is the carbon bond-length in a carbon nanotube. The charge density on this triangular area can be written as $d = \frac{qi}{s}$. The electric potential at the center of the triangle, i.e. the atom i, is resulted from the uniformly distributed charge and can be expressed as [55]

$$V(r_i)_i = \iint_s \frac{q_i/s}{4\pi\epsilon_0\sqrt{\xi+\eta}}\, d\xi\, d\eta. \tag{2.29}$$

The diagonal term extracted from (2.29) is

$$a_{ij} = \frac{1}{4\pi\epsilon_0 s} \iint_s \frac{1}{\sqrt{\xi+\eta}}\, d\xi\, d\eta \tag{2.30}$$

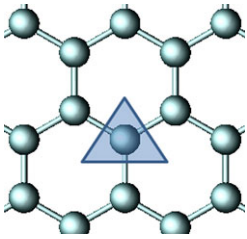


Fig. 2.14 Electric charge distributed on a triangular area surrounding a carbon atom

which has a closed form expression as

$$a_{ij} = \frac{b\sqrt{3}\ln(2+\sqrt{3})}{4\pi\epsilon_0 s}. \tag{2.31}$$

4 Conclusion

The objective of this chapter was to interface multiscale simulation tools with real-time truly virtual reality techniques for bio-nano robotic prototyping at the design stage. Molecular modeling is advocated here as a key methodology for research and development since it predicts the nanoscale interaction of unfamiliar combinations of biological and inorganic materials, and evaluates strategies for designing nanostructures for nanotechnological uses. The ability to interact with a computer-generated object in the same manner that a person would interact with a physical object—to investigate its structure by simply moving around it, to change its position by grabbing the object and moving the hand in space, without such artificial devices as computer mice. The design and prototyping methodology is illustrated in this chapter through the proposition of two case studies.

The first one involves multiscale modeling tools (quantum mechanics, molecular dynamics, continuum mechanics) coupled to virtual reality advanced techniques. In order to design and evaluate the characteristics of molecular robots, we proposed nanophysics-based simulation coupled to multimodality perception and real time computation. We have introduced a collection of utilities and programming libraries aimed at enhanced sampling and multiscale modeling applications in structural biology and nanotechnology. The tool set interfaces with the standard quantum and semi-empirical PM3 or Hartree-Fock molecular orbital models, molecular modeling packages for all-atom modeling, and elastic continuum models for structure design. We have built many software components and used virtual reality interfaces which together constitute an implementation of this interactive multiscale simulation platform. Design, simulation, and control of novel bio-nano structures, actuators and robotic systems are developed in Chap. 3 in order to illustrate the proposed interactive multiscale prototyping platform.

The second one integrates a co-prototyping approach based on a dual paradigm, i.e., experimentation and molecular modeling. Usually, nanodevice optimization is only based on experimental investigation of nanodevice characteristics. As all design parameters are not accessible by experimental measurements, the designer is not able to characterize deeply the nanodevice operating principles leading to optimal performances. As alternative, we propose to use jointly modeling tools to support the designer in order to characterize novel phenomenons, evaluate energy densities or new operational principles. The proposed modeling methods uses electrostatic calculation methods with classical molecular dynamics with AIREBO potential. The cooperative work between experiments and simulation paves the way for high-performance nanorobotic components. As illustration of this concept, a co-prototyping methodology applicable to optimized multiwalled carbon nanostructures is proposed in Chap. 4.

References

1. Kitamura, K., Tokunaga, M., Iwane, A.H., Yanada, A.: A single myosin head moves along an actin filament with rectangular steps of 5.3 nm. Nature **397**, 129 (1999)
2. Shingyoji, C., Higuchi, H., Yoshimura, M., Katayama, E., Yanagida, T.: Dynein arms are oscillating force generators. Nature **393**, 711–714 (2001)
3. Montegano, C.D., Bachand, G.D.: Constructing nanomechanicaldevices powered by biomolecular motors. Nanotechnology **10**, 225–331 (1999)
4. Erickson, H.P.: Stretching single protein molecules: titin as a wired spring. Science **276**, 1090–1092 (2003)
5. Mahadevan, L., Matsudaira, P.: Mobility powered by supramolecular, springs and ratchets. Science **288**, 95–99 (2000)
6. Hamdi, M., Sharma, G., Ferreira, A., Mavroidis, D.: Characterization of protein based spring-like elastic joints for biorobotic applications. In: IEEE International Conference on Robotics and Automation, May 15–19, Orlando, FL, pp. 1794–1799 (2006)
7. Ferreira, A., Sharma, G., Mavroidis, D.: New trends in bionanorobotics using virtual reality technologies. In: IEEE International Conference on Robotics and Biomimetics, June 30–July 3, Hong Kong, pp. 89–94 (2005)
8. Requicha, A.: Nanorobots, NEMS nanoassembly. IEEE J. Sens. **91**(11), 1922–1933 (2003)
9. Li, G.Y., Xi, N., et al.: "Videolized" atomic force microscopy for interactive nanomanipulation and nanoassembly. IEEE Trans. Nanotechnol. **4**(5), 605–615 (2004)
10. Shih, C.-Y., Zheng, S., Meng, E., Tai, Y.-C., Liu, Y., Stoddart, J.F.: Nano-to-micro self-assembly using shear flow devices. In: 17th IEEE International Conference on Micro Electro Mechanical Systems, pp. 422–425 (2004)
11. Yin, P.: DNA based self-assembly and nano-device: theory and practice. Doctoral Thesis, UMI Order Number: AAI3181510, Duke University, 2005
12. Humphrey, W., Dalke, A., Schulten, K.: VMD: visual molecular dynamics. J. Mol. Graph. **14**, 33–38 (1996)
13. Taylor, R.M. II: VRPN: virtual reality peripheral network. http://www.cs.unc.edu/Research/vrpn/
14. Stone, J., Gullingstrud, J., Grayon, P., Schulten, K.: A system for interactive molecular dynamics simulation. In: 2001 ACM Symposium on Interactive 3D Graphics, ACM SIGGRAPH, New York, pp. 191–194 (2001)
15. Nelson, M., Humphrey, W., Gursoy, A., Dalke, A., Kale, L., Skeel, R.D., Schulten, K.: NAMD-a parallel object-oriented molecular dynamics program. Int. J. Supercomput. Appl. High Perform. Comput. **10**, 251 (1996)
16. MacKerell, A.D., Bshford, D., Bellott, M., Dunbrack, R.L., Evanseck, J.D., Field, M.J., et al.: All-atom empirical potential for molecular modeling and dynamics studies of proteins. J. Phys. Chem. B **102**, 3586–3616 (1998)
17. Maiti, A.: Multiscale modeling with carbon nanotubes. Microelectron. J. (2007)
18. Liu, Y.J., Chen, X.L.: Continuum models of carbon nanotube-based composites using the boundary element method. J. Bound. Elem. **1**(2), 316–335 (2003)
19. Karakasidis, T.E., Charitidis, C.A.: Multiscale modeling in nanomaterials science. Mater. Sci. Eng. (2006)
20. Ghoniem, N.M., Busso, E.P., Kioussi, N., Huang, H.: Multiscale modelling of nanomechanics and micromechanics: an overview. Philos. Mag. **83**(31–34), 3475–3528 (2003)
21. Feig, M., Karanicolas, J., Brooks, C.L.: MMTSB Tool Set: enhanced sampling and multiscale modeling methods for applications in structural biology. J. Mol. Graph. Model. **22**, 377–395 (2004)
22. Ahmed, A., Gohlke, H.: Multiscale modeling of macromolecular conformational changes combining concepts from rigidity and elastic network theory. Proteins Struct. Funct. Bioinf. **63**, 1038–1051 (2006)
23. Villa, E., Balaeff, A., Schulten, K.: Structural dynamics of the lac repressor-DNA complex revealed by a multiscale simulation. Proc. Natl. Acad. Sci. USA **102**(19), 6783–6788 (2005)

24. Lai-Yen, S.K., Lee, Y.S.: Energy-field optimization and haptic-based molecular docking and assembly search system for computer-aided molecular design (CAMD). In: Symposium on Haptic Interfaces for Virtual Environment and Teleoperator Systems, pp. 233–240 (2006)
25. Pattabiraman, N., Levitt, M., Ferrin, T.E., Langridge, R.: Computer graphics in real-time docking with energy calculation and minimization. J. Comput. Chem. **6**(5), 432–436 (1986)
26. Gao, M., Wilmanns, M.: Steered molecular dynamics study of titin I1 domain unfolding. Biophys. J. **83**, 3435–3445 (2002)
27. Hamdi, M., Sharma, G., Ferreira, A., Mavroidis, D.: Molecular mechanics study on bio-nano robotic components using force-feedback. In: IEEE International Conference on Robotics and Biomimetics, June 30–July 3, Hong Kong, pp. 105–110 (2005)
28. Wollacott, A.M., Merz, K.M.: Haptic applications for molecular structure manipulation. J. Mol. Graph. Model. **25**(6), 801–805 (2007)
29. Daunay, B., Micaelli, A., Régnier, S.: 6 DOF haptic feedback for molecular docking using wave variables. In: IEEE International Conference on Robotics and Automation, May, Roma, Italy (2007)
30. Stewart, J.J.P.: Optimization of parameters for semi-empirical methods IV: extension of MNDO, AM1, and PM3 to more main group elements. J. Mol. Model. **10**, 155–164 (2004)
31. Cramer, C.J.: Essentials of Computational Chemistry, pp. 191–232. Wiley, New York (2002)
32. Kuhn, B., Kollman, P.A.: Binding of a diverse set of ligands to avidin and streptavidin: an accurate quantitative prediction of their relative affinities by a combination of molecular mechanics and continuum solvent models. J. Med. Chem. **43**, 3786–3791 (2000)
33. MacKerell, Jr. A.D., Banavali, N., Foloppe, N.: Development and current status of the CHARMM force field for nucleic acids. Biopolymers **56**, 257–265 (2001)
34. Reference, Monte-Carlo
35. Trombitas, K., Gasser, M., Labeit, S., Jin, J.-P., Kellermayer, M., Helmes, M., Granzier, H.: Titin extensibility in situ: entropic elasticity of permanently folded and permanently unfolded molecular segments. J. Cell Biol. **140**, 853–859 (1998)
36. Zhang, B., Guangzhao, X., Evans, J.S.: A kinetic molecular model of the reversible unfolding and refolding of Titin under force extension. Biophys. J. **77**, 1306–1315 (1999)
37. Isralewitz, B., Baudry, J., Gullingsrud, J., Kosztin, D., Schulten, K.: Steered molecular dynamics investigations of protein function. J. Mol. Graph. Model **19**(12), 13–25 (2001)
38. Hohenberg, P., Kohn, W.: Phys. Rev. B **136**, 864 (1964)
39. Kohn, W., Sham, L.J.: Phys. Rev. A **140**, 1133 (1965)
40. Cramer, C.J.: Essentials of Computational Chemistry. Wiley, New York (2002)
41. Goringe, C.M., Bowler, D.R., Hernández, E.: Rep. Prog. Phys. **60**, 1447 (1997)
42. Rapaport, D.C.: The Art of Molecular Dynamics Simulation. Cambridge University Press, Cambridge (1995)
43. Allen, M.P., Tildesley, D.J.: Computer Simulation of Liquids. Clarendon, Oxford (1987)
44. Tersoff, J.: Phys. Rev. Lett. **56**, 632 (1986)
45. Tersoff, J.: Phys. Rev. B **27**, 6991 (1988)
46. Tersoff, J.: Phys. Rev. B **39**, 5566 (1989)
47. Brenner, D.W.: Phys. Rev. B **42**, 9458 (1990)
48. Stuart, S.J., Tutein, A.B., Harrison, J.A.: J. Chem. Phys. **112**, 6472 (2000)
49. Abell, G.: Empirical chemical pseudopotential theory of molecular and metallic bonding. Phys. Rev. B **31**, 6184 (1985)
50. Brenner, D.W.: The art and science of an analytic potential. Phys. Stat. Sol. (B) **217**, 23 (2000)
51. Robertson, D.H., Brenner, D.W., White, C.T.: On the way to fullerenes: molecular dynamics study of the curling and closure of graphitic ribbons. J. Phys. Chem. **96**, 6133–6135 (1992)
52. Iijima, S., et al.: Structural flexibility of carbon nanotubes. J. Chem. Phys. **104**, 2089 (1996)
53. Huhtala, M., Kuronen, A., Kaski, K.: Carbon nanotubes under bending strain. Mater. Res. Soc. Symp. Proc. **706**, 289–294 (2002)
54. Pettifor, D.G., Oleinik, I.I.: Analytic bond-order potentials beyond Tersoff-Brenner. Phys. Rev. B **59**, 8487–8506 (1999)
55. Li, C.Y., Chou, T.W.: Electrostatic charge distribution on single-walled carbon nanotubes. Appl. Phys. Lett. **89**, 063103 (2006)
56. Hamdi, M., Ferreira, A.: DNA nanorobotics, Microelectron. J. (2008, in press)



http://www.springer.com/978-90-481-3179-2

Design, Modeling and Characterization of Bio-Nanorobotic Systems

Hamdi, M.; Ferreira, A.

2011, XXVII, 158 p., Hardcover
ISBN: 978-90-481-3179-2